General Three-Phase Relative Permeability Model for Prudhoe Bay

G.R. Jerauld, SPE, Arco E&P Technology

Summary

This paper describes two- and three-phase relative permeability concepts important for Prudhoe Bay. It includes a three-phase relative permeability correlation that incorporates hysteresis in gas, oil, and water relative permeability as well as the dependence of relative permeability on composition and gas/oil interfacial tension (IFT). The functional forms chosen to correlate the relative permeability data were based on interpretation of the pore-level mechanisms that determine fluid flow. The three-phase correlation reduces to traditional models in various limits and is more consistent with available data and trends in the literature than previous correlations. Although this correlation was developed for Prudhoe Bay, it can be and has been applied to other mixed-wet reservoirs with changes in the input parameters. The correlation is particularly useful in situations where both compositional effects and hysteresis are important.

Introduction

The ultimate use of relative permeability models is to help design, optimize, and analyze oil-displacement processes. Clearly, relative permeability is just one part of the recovery picture; reservoir characterization, gravitational effects, phase behavior, and mass transfer processes among other factors all interact to determine the amount of oil that can be recovered economically. Nevertheless, relative permeability plays a central role. The primary impact of relative permeability on process design is through fluid mobilities and fractional flows. Total fluid mobilities determine the resistance to flow of the fluids and hence affect (1) injectivity and the overall timing of the process and (2) the severity of viscous fingering or channeling and the "robustness" of a process to heterogeneities in general. The fractional flows impact producing-water/-oil ratio, producing-gas/-oil ratio, breakthrough timing, and ultimate and incremental recoveries. The magnitude and location of waterflood residual oil, the target for the enhanced oil recovery (EOR) process, is impacted by low-capillary-number relative permeability. Waterflood oil recovery is also affected by the presence of gas through its impact on water/oil relative permeability ratio as in immiscible water-alternating-gas (WAG) processes or in waterflooding where oil was forced into regions previously invaded by an expanded gas cap. Residual oil to gas in gravity drainage is determined primarily by oil/gas relative permeability, which in turn is impacted by the level of initial water saturation. Although phase-behavior mechanisms (attainment of miscibility, stripping of oil by gas, or swelling of oil by gas) are important mechanisms in developed miscible flooding, capillary number effects could also play a role because the IFT between the oil and gas becomes low as miscibility is approached.

In general, the relative permeability of a phase is a function of five factors: saturation of the phases, saturation history, wettability, pore structure, and capillary number. It is clear, therefore, experimental data are insufficient to cover all scenarios and that a relative permeability model, based on a physical concept of how fluids flow, is required both to extend the range of experimental data and to approximate relative permeability in simulations efficiently. The three-phase correlation presented in this paper is intended to be a relatively simple model that incorporates the basic trends in available data and rudimentary physical concepts. The relative permeability curves given are "rock curves" that apply to the core-scale and may not give accurate results in simulations with gridblocks of tens or hundreds of feet.

Original SPE manuscript received for review 23 February 1997. Revised manuscript received 6 August 1997. Paper peer approved 24 August 1997. Paper (SPE 36178) first presented at the 1996 Abu Dhabi International Petroleum Exhibition and Conference held in Abu Dhabi, 13–16 October.

Prudhoe Bay is a mixed-wet sandstone reservoir. The Sadlerochit formation, which makes up most of the producing interval, is composed of high-permeability fluvial sands and interbedded shales with a high net-to-gross. The sands contain a significant fraction of microporous chert as well as quartz sand and a small amount of Kaolinite clay. The model described later was designed for all the major recovery processes that occur in Prudhoe (gravity drainage, waterflooding, miscible gas injection) and the interaction between these processes.

Two-Phase Relative Permeability

Gas Trapping. The trapped-gas saturation influences water injectivity and the amount of diversion of water in WAG processes and is a primary determinant of the amount of miscible injectant retained in the reservoir and unavailable for oil displacement. The trapped-gas data for Prudhoe Bay (**Fig. 1**) are poorly fit by the Land[18] equation but are reasonably well approximated by a modified form,

$$S_{gt}\left(S_g^{\max}\right) = \frac{S_g^{\max}}{1 + \left(1/S_{gr} - 1\right)\left(S_g^{\max}\right)^{1 + bS_{gr}/\left(1 - S_{gr}\right)}}, \quad \ldots\ldots\ldots (1)$$

where $S_g^{\max}$ = maximum gas saturation that has occurred at that location and S_{gr} (S_{gt} at $S_g^{\max} = 1$) and b are empirically derived constants (Land's equation has $b = 0$). This equation embodies the idea that the maximum gas saturation determines the amount of trapping in multicycle processes. This modification preserves the simplest constraints for physically consistency: (1) trapped-gas saturation is always less than maximum gas saturation and (2) trapped-gas saturation approaches the maximum saturation at low maximum gas saturations. In addition, because ordinary mechanisms do not lead to a decrease in trapped-gas saturation with an increase in maximum gas saturation, this curve should not have a negative slope, which corresponds to $b \leqq 1$. Taking $b =$ one, corresponding to a zero slope at $S_g^{\max} = 1$, yields a single parameter equation that best fits Prudhoe data.

Measurements show no difference between laboratory and reservoir conditions in both gas relative permeability and trapped gas. Studies in the literature[11-13] also indicate that temperature and pressure do not affect the level of trapped gas. Comparison of trapping of gas by water or oil both when two and three phases were present give essentially the same result. Moreover, tests on individual plugs and their composites showed that the average of the plugs matches the composite values to within the accuracy of the measurements. In-situ saturation monitoring gives centimeter-scale values for trapped-gas saturation consistent with the core-plug values.

Gas Relative Permeability. Gas relative permeability influences the propensity of gas to propagate preferentially down higher-permeability layers as opposed to sweeping the reservoir efficiently. Gas relative permeability is well represented by **Fig. 2** and

$$k_{rg} = \frac{\left(1 + c_{g2}\right)\left[S_g - S_{gt}\left(S_g^{\max}\right)/\left(1 - S_{gr}\right)\right]^{c_{g1}}}{1 + c_{g2}\left[S_g - S_{gt}\left(S_g^{\max}\right)/\left(1 - S_{gr}\right)\right]^{c_{g1}\left(1 + 1/c_{g2}\right)}}, \quad \ldots . (2)$$

where c_{g1} and c_{g2} are empirically derived constants and the trapped-gas saturation is given by Eq. 1. At low gas saturations, the numerator of this equation dominates and Eq. 2 approaches the conventional Corey equation.[7] At high gas saturations, the second term of the denominator becomes dominant and causes a continuously decreasing slope of the k_{rg} curve (see Fig. 2). This behavior is consistent with the idea that gas enters larger pores first and then successively smaller pores. The numerator models the way a fluid phase becomes connected across the sample (i.e. the dependence of relative perme-

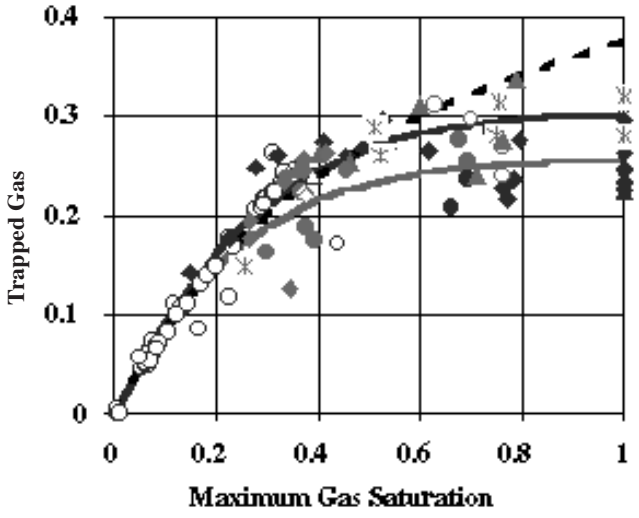

Fig. 1—Trapped-gas data for the Sadlerochit: bold solid lines = "zero-slope" Land equation and dashed = ordinary Land.

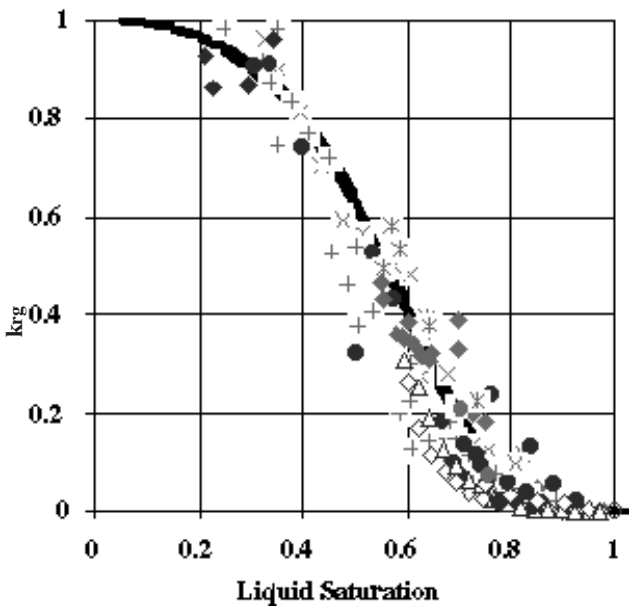

Fig. 2—Comparison of primary-drainage nonwetting-phase relative permeability data with correlation. Data are from steady-state (solid circles), pseudosteady-state (x, +,*) and low-rate displacements on composites corrected for capillary end effects (diamonds). Gas/water, gas/oil, and water-wet oil/water relative permeabilities are the same to within experimental accuracy.

ability of a phase on the size and shape of the connected set of pores filled by that phase). The denominator of Eq. 2 represents the diminishing contributions of successively smaller pores to the relative permeability and is designed to give a zero slope at $S_g = 1$. The hysteresis behavior is the same as Carlson's.[5] Imbibition and drainage relative permeability are related through the gas-trapping function (Eq. 1). Evidence in the literature[15] and Prudhoe Bay data indicate that no hysteresis occurs between imbibition and secondary drainage.[13] Most gas relative permeability reported in the literature is independent of the other two-phase saturations.[3,10] In light of this and because it is impossible to distinguish between gas/water (with and without S_{orm}) and gas/oil (with and without S_{wc}) relative permeability on the basis of available data, the same function is used in two- and three-phase immiscible flow.

Unlike CO_2 studies,[9,26] Prudhoe experiments show that no difference exists between reservoir-condition hydrocarbon miscible injectant (MI) and ambient nitrogen relative permeability both in imbibition and in secondary drainage. Other experiments show no difference between primary-drainage gas relative permeability of laboratory fluids (N_2/water or refined oil) at ambient conditions and MI at reservoir conditions. A comparison of the properties of various fluids and MI (mixture of approximately 21 mol% CO_2, 33% methane, 20% ethane, 22% propane, and 4% butane) given in **Table 1** shows that it is unclear whether MI is gas- or liquid-like, so this observation is a useful bound in understanding compositional dependence.

Oil/Water Relative Permeability. Prudhoe Bay is a mixed-wet reservoir that displays a wettability transition within the reservoir, more water-wet behavior being associated with higher initial water saturations.[13] This complicates the oil/water relative permeability model, introducing a change in the shape of the curves with changing initial water saturation in addition to the usual dependence on minimum water saturation.

TABLE 1—FLUID PROPERTIES AT RESERVOIR AND LABORATORY CONDITIONS

			Conditions	
Fluid	density (gm/cm^3)	viscosity (cp)	Temperature (°F)	Pressure (psi)
Live Oil	0.767	1.21	200	3,500
Lean Gas	0.212	0.0255	200	3,500
MI	0.368	0.0404	200	3,500
Methane	0.134	0.0189	200	3,500
Nitrogen	0.039	0.0185	77	500

The initial water saturation dependence is based on the idea that the system is mixed-wet and, therefore, that the minimum water saturation determines the scanning curve. For a given piece of rock, Salathiel[24] argues that during primary drainage, oil enters the rock and displaces water, starting with the largest pores first. Adsorption of components onto the rock renders some of the oil-contacted parts of the pores oil-wet. Thus, the higher the initial oil saturation, the greater the fraction of pores rendered oil-wet. For a given water saturation, water occupies more large pores during imbibition than in primary drainage because many large pores become oil-wet during primary drainage. In primary drainage, water is strongly wetting and, thus, occupies the smallest pores. Therefore, water relative permeability is larger in imbibition than primary drainage at a given water saturation level and lower levels of initial water saturation lead to larger levels of imbibition relative permeability. Conversely, oil relative permeability is larger in primary drainage than imbibition and decreases more rapidly for lower initial water saturations.

Two-phase imbibition oil relative permeability is well fit by the Corey model[7]; i.e.,

$$k_{row}(1 - S_w) = k_{ocw}\left[\frac{1 - S_w - S_{otw}(S_w^{\min})}{1 - S_w^{\min} - S_{otw}(S_w^{\min})}\right]^{c_{ow1}}, \quad \ldots\ldots (3)$$

where the residual oil to waterflooding is given by

$$S_{otw}(S_w^{\min}) = \frac{(1 - S_w^{\min})}{1 + (1/S_{orw} - 1)(1 - S_w^{\min})^{1/(1 - S_{orw})}} \quad \ldots\ldots (4)$$

and $S_w^{\min}$ = minimum water saturation, S_{orw} = maximum residual oil saturation (ROS), i.e. for $S_w^{\min} = 0$. Minimum water saturation is used rather than initial water saturation because, in simulations involving transition zones, water saturation can become forced lower than the initial value (**Fig. 3**). The Corey exponent, c_{ow1}, decreases as $S_w^{\min}$ increases and approaches strongly wetting values (≈ 1.2 to 1.6) as $S_w^{\min}$ approaches one. The oil relative permeability at initial water saturation is found by analogy from gas relative permeability (Eq. 2) and has the same form.

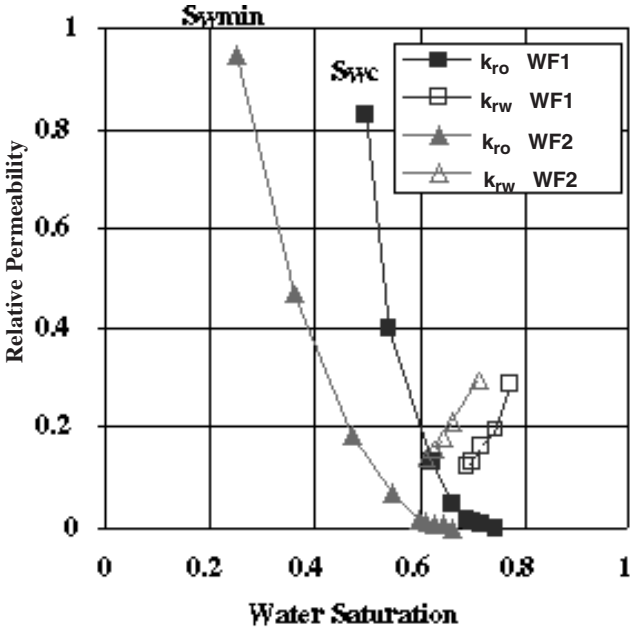

Fig. 3—Relative permeability measured on uninvaded core (WF1) and after re-establishing a lower initial water saturation (WF2).

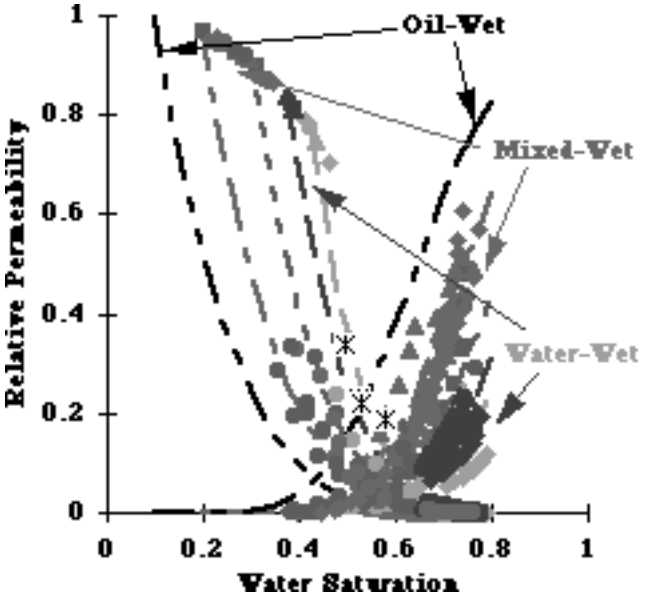

Fig. 4—Laboratory relative permeability data for Prudhoe Bay; bold solid lines = correlation for various initial water saturations (S_{wc} = 0.1, 0.2, 0.3, 0.38, 0.43) and stars = water relative permeability endpoints measured in wettability tests on upstructure plugs.

To fit imbibition water relative permeability, a more S-shaped rather than a simple Corey model is required (**Fig. 4**), namely

$$k_{rwo} = \frac{\left(1 + c_{wo5}\right)\left[\left(S_w - S^*_{wro}\right)/\left(1 - S^*_{wro}\right)\right]^{c_{wo4}}}{1 + c_{wo5}\left[\left(S_w - S^*_{wro}\right)/\left(1 - S^*_{wro}\right)\right]^{c_{wo4}}}, \quad \ldots\ldots\ldots (5)$$

where c_{wo5} decreases as minimum water saturation increases and approaches zero as $S_w^{\min}$ approaches unity. The effective irreducible water saturation, S^*_{wro}, is introduced so that the water relative permeability predicted by Eq. 6 at $S_w^{\min}$ matches the primary-drainage value (Eq. 9); i.e.,

$$S^*_{wro} = \left(S_w^{\min} - S^{n*}_{wro}\right)/\left(1 - S^{n*}_{wro}\right), \quad \ldots\ldots\ldots\ldots\ldots (6)$$

where $S^{n*}_{wro} = \left\{k^{PD}_{rw}/\left[1 + \left(1 - k^{PD}_{rw}\right)a\right]\right\}^{1/c_{wo4}}$ . . . . . (7)

and the water relative permeability at initial water saturation is

$$k^{PD}_{rw} = \left(S_w^{\min}\right)^{c_{w1}} \quad \ldots\ldots\ldots\ldots\ldots\ldots\ldots\ldots\ldots (8)$$

and is found from water relative permeability measured for strongly wetting systems, usually a gas/water experiment.

The initial water saturation dependence of this correlation was constructed to reproduce the ROS's estimated from water-based core data for the range of initial water saturations occurring at Prudhoe Bay.[13] In addition, waterfloods run on core not invaded by drilling fluid have been rerun after the cores were centrifuged to a water saturation below the initial level and show hysteresis behavior consistent with this model (Fig. 3). Relative permeability at initial water saturation is consistent with initial water cuts measured on wells in the transition zone. This correlation (Eqs. 3 and 6) assumes that no hysteresis occurs between imbibition and secondary drainage. Two separate studies showed hysteresis small enough to be within the range of experimental uncertainty.

Water/Gas Relative Permeability. Prudhoe data generally support the assumption that all the two-phase liquid relative permeabilities (oil and water) are the same for the oil/gas and water/gas systems. In addition, steady-state gas/water relative permeability experiments show that water relative permeability is approximately the same in the presence of residual oil to miscible flood whether the gas is miscible injectant (MI) at reservoir conditions or nitrogen at ambient conditions in both secondary drainage and imbibition. These observations are in accord with data in the literature for strongly-wetting systems.[13,15] Water is strongly wetting with respect to gas and, therefore, will have little hysteresis. Water relative permeability has the same form and is essentially the same as the primary-drainage water relative permeability (Eq. 9) in the water/oil system but is much different than imbibition relative permeability in the water/oil system. Equations for oil relative permeability in the gas/oil system are given later.

Compositional Effects

Capillary Number Dependence. A great body of evidence indicates that trapping behavior and relative permeability depend on the ratio of flow rate to interfacial tension (IFT) at low enough IFT's or high enough flow rates.[1,2,4,17] Because low IFT's occur near the miscible front in the multicontact miscible gas process, a complete model must include this mechanism. The dimensionless group that measures the regime of behavior is the capillary number,

$$N_c = k\|\nabla p\|/\sigma\,, \quad \ldots\ldots\ldots\ldots\ldots\ldots\ldots\ldots (9)$$

where k = absolute permeability, ∇p = pressure gradient, and σ = IFT.

Fig. 5 compares how residual oil to waterflooding varies with capillary number for Prudhoe[16] and literature[17] data. Trapped oil in a waterflood of a water-wet rock is usually comparable with the trapped gas in gas/oil displacement. Fig. 5 also shows a capillary desaturation curve for Berea sandstone measured in our laboratory that exhibits complete desaturation at much lower capillary numbers than the Prudhoe data. While it is possible that the long tail is caused by artifacts in interpretation of the centrifuge experiments or incomplete cleaning of the rock, a possible explanation for the long-tailed nature of the capillary desaturation curve in the Prudhoe sample is its broad pore-size distribution. Because the capillary force required to mobilize residual oil from a pore is larger for smaller pore sizes, desaturating occurs at higher capillary numbers. However, gas is not trapped in micropores,[13] so the capillary number required for zero trapping of gas is significantly smaller than for mobilizing oil from micropores. The number of orders of magnitude drop in IFT to mobilize all the gas should be approximately the same as sandstone with similar macropores, or approximately two orders of magnitude. It is clear that gas is not trapped in micropores because the trapped-gas saturation does not increase with maximum gas saturation above maximum values of approximately 0.4. Moreover, simulations indicate that gas sat-

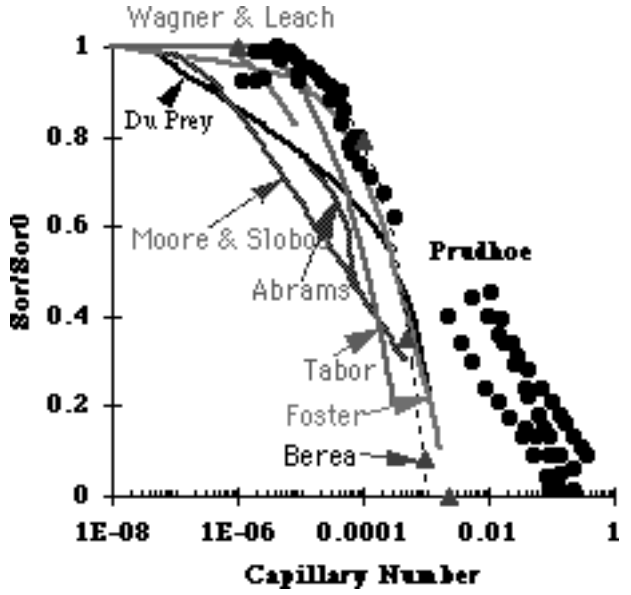

Fig. 5—Capillary desaturation curves from literature[17] and reported for Prudhoe.[16] Triangles connected by a dashed line are data measured by our laboratory on Berea sandstone corresponding to data in Fig. 6.

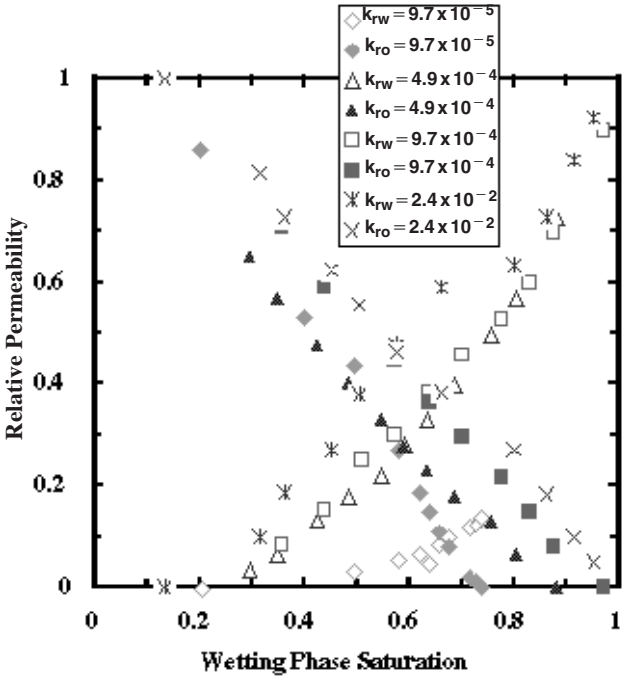

Fig. 6—Capillary number dependence of steady-state relative permeability measured in fired and acidized Berea sandstone.

urations typically do not exceed 0.4 in the miscible process and, therefore, no gas enters the micropores. Most field and laboratory waterfloods are conducted at capillary numbers less than 10^{-6}, so desaturation of the oil by water does not occur by this mechanism.

The reduction in nonwetting phase saturation, S_{nr}, with increasing capillary number is well represented by

$$\frac{S_{nr}}{S_{nr}^0} \equiv \theta = \max\left\{\min\left[(1/e)\log\left(N_c/N_c^{knee}\right), 1\right], 0\right\}, \quad \ldots\ldots\ldots (10)$$

where $1/e$ = number of order of magnitudes decrease in IFT required for zero residual and N_c^{knee} = capillary number where reduction from S_{nr}^0 starts.

As the capillary number increases, relative permeability curves move from immiscible limits toward straight lines. **Fig. 6** shows constant capillary number data taken in our laboratory with strongly wetting fluids in Berea sandstone. Analysis indicates that the capillary desaturation curve can be used to scale the relative permeability curvatures as miscibility is approached. The capillary number dependence of the oil relative permeability Corey exponent in the gas/oil system may be approximated as

$$c_{og1} = c_{og1}^{toe} + \left(c_{og1}^{knee} - c_{og1}^{toe}\right)\theta, \quad \ldots\ldots\ldots\ldots\ldots\ldots (11)$$

where the "toe" value of c_{og1} corresponds to the high capillary number limit where the residual nonwetting phase saturation is zero (i.e., low IFT) and the "knee" value corresponds to the low capillary-number limit (i.e., high IFT) below which the ROS does not increase. Frequently, the Corey exponent approaches one as miscibility is approached. Similar scaling is applied to gas relative permeability in the gas/oil system, as Fig. 6 indicates.

Rough estimates of when IFT effects are important can be generated from the capillary desaturation curve above if one uses approximate field flow rates and physical properties. Very near the wellbore where pressure gradients are larger, the IFT at which relative permeability curves approach the miscible limit is larger. On the basis of the capillary desaturation curve used in Fig. 5, capillary number effects become important for IFT's less than 0.1 dyne/cm on when oil viscosity is ≈ 1 cp, frontal velocity is 1 ft/D, porosity is 23%, and a capillary number at the knee is 10^{-5}. On the basis of the previous discussion, the relative permeabilities should be close to straight lines if the IFT becomes two orders of magnitude lower or below an IFT of 0.001 dyne/cm. Live-oil/gas IFT was approximately 2 to 3 dynes/cm at initial reservoir conditions and increased as reservoir pressure dropped. Therefore, capillary number effects may become important if the IFT diminishes by more than an order of magnitude from the initial value. Live-oil/water IFT is much larger, 25.3 ± 0.3 dynes/cm, so oil/water capillary number effects are unimportant.

Compositional Consistency. The concept of compositional consistency applies to simulation of compositional processes (i.e., those where the compositions of phases change and where phases disappear and reappear owing to changes in composition).* The idea is that the relative permeability of a hydrocarbon phase should not depend on whether it is labeled "oil" or "gas" by the simulator but should depend instead on the composition or physical properties of the phase and its saturation. Problems with compositional consistency generally occur in three-phase situations when it becomes unclear whether a hydrocarbon phase is gas or oil. A simple test of a model is to imagine a two-phase situation entailing water and a hydrocarbon phase and to ask whether the model has a continuously varying hydrocarbon relative permeability as the hydrocarbon varies from gas to oil. Such a dependency is important both to estimate relative permeability accurately and for simulator stability.

A key requirement of compositional consistency is that at miscibility,

$$k_{ri} = \frac{S_i}{(1 - S_w)} k_{rhw}(S_w), \quad \ldots\ldots\ldots\ldots\ldots\ldots\ldots (12)$$

where i = either oil or gas and k_{rhw} = hydrocarbon relative permeability in a hydrocarbon/water system. Because of the dependence of wettability on composition, k_{rhw} depends on the composition of the hydrocarbon.* In addition, there should be a single water relative permeability at miscibility, independent of the saturation of gas or oil. These conditions are necessary because the split between gas and oil becomes arbitrary as their compositions approach each other.

To accomplish this it is necessary to define a measure of composition. There are many possible measures of composition (e.g., the density of the phase). A convenient choice is the parachor-weighted molar density,* ξ, which is usually available in a compositional simulator because it is used to estimate the IFT.[23] A typical parachor

*Personal communication with A.A. Zick, Improved Recovery Technologies, San Francisco (1989).

molar density of an immiscible gas is less than 70, while oil is greater than 130 and MI is 80. It is useful to introduce a dimensionless measure of the oil-like, as opposed to gas-like, character of a phase.

$$f_h = \max\left(\min\left\{\left[\left(\xi_h - \xi_{gi}\right)/\left(\xi_{oi} - \xi_{gi}\right)\right], 1\right\}, 0\right), \quad \ldots\ldots\ldots (13)$$

where ξ_{gi} and ξ_{oi} = parachor-weighted molar density of immiscible gas and oil, respectively. This function is used to interpolate hydrocarbon and water relative permeabilities between oil/water and gas/water limits to reflect the different wettabilities of these phase pairs.

Hydrocarbon/Water Scanning. Comparison of the gas and oil equations shows that they can be combined into a single, hydrocarbon hysteresis model to yield

$$k_{rhw} = \frac{\left(1 + c_{hw2}\right)S_1^{c_{hw4}}S_2^{c_{hw1}}}{1 + c_{hw2}S_1^{c_{hw6}}S_2^{c_{hw3}}}, \quad \ldots\ldots\ldots (14)$$

where $S_1 = \left\{\left[S_{hw}^{\max} - S_{htw}\left(S_{hw}^{\max}\right)\right]/\left(1 - S_{hrw}\right)\right\}, \quad \ldots\ldots\ldots (15)$

$$S_2 = \left\{\left[1 - S_w - S_{htw}\left(S_{hw}^{\max}\right)\right]\left[/S_{hw}^{\max} - S_{htw}\left(S_{hw}^{\max}\right)\right]\right\}, \quad \ldots\ldots (16)$$

and $S_{htw} = \dfrac{S_{hw}^{\max}}{1 + \left(1/S_{hrw} - 1\right)\left(S_{hw}^{\max}\right)^{1/\left(1 - S_{hrw}\right)}} \quad \ldots\ldots\ldots (17)$

and where the maximum hydrocarbon saturation is determined from the following equations.

$$S_{hw}^{\max} = \max\left[1 - S_w, S_g^{\max} + f_h\left(1 - S_w^{\min} - S_g^{\max}\right)\right]. \quad \ldots\ldots (18)$$

The hydrocarbon parameters are interpolated compositionally:

$$S_{hrw} = \left(1 - f_h\right)S_{gr} + S_{orw}, \quad \ldots\ldots\ldots (19)$$

$$c_{hw1} = \left(1 - f_h\right)c_{g1} + f_h c_{ow1}, \quad \ldots\ldots\ldots (20)$$

$$c_{hw2} = \left(1 - f_h\right)c_{g2} + f_h c_{ow2}, \quad \ldots\ldots\ldots (21)$$

$$c_{hw3} = \left(1 - f_h\right)c_{g1}\left(1 + 1/c_{g2}\right), \quad \ldots\ldots\ldots (22)$$

$$c_{hw4} = \left(1 - f_h\right)c_{g1} + f_h c_{ow4}, \quad \ldots\ldots\ldots (23)$$

$$c_{hw6} = \left(1 - f_h\right)c_{g1}\left(1 + 1/c_{g2}\right) + f_h c_{ow6}, \quad \ldots\ldots\ldots (24)$$

and $S_g^{\max} = \max\left[\left(1 - f_g\right)S_g + \left(1 - f_o\right)S_o, S_g^{\max}, S_{gt}^{-1}\left(S_{gc}\right)\right].$

$$\ldots\ldots\ldots (25)$$

The critical gas saturation is $S_{gc} = 0.038$ on the basis of an average of laboratory data. Because water relative permeability is different in the water/oil and water/gas systems, a correlation for water relative permeability is also needed.

In the oil/water system it is the minimum water saturation that determines that pores are exposed to oil and therefore become intermediate or oil-wet. On the other hand, water is usually strongly wetting with respect to gas and will have little hysteresis. Therefore, a convenient form for the water relative permeability is

$$k_{rwh} = \frac{\left(1 + c_{wh5}\right)\left[\left(S_w - S_{wrh}^*\right)/\left(1 - S_{wrh}^*\right)\right]^{c_{wh4}}}{1 + c_{wh5}\left[\left(S_w - S_{wrh}^*\right)/\left(1 - S_{wrh}^{n*}\right)\right]^{c_{wh4}}} \quad \ldots\ldots\ldots (26)$$

where $S_{wrh}^* = \left[\left(S_w^{\min} - S_{wrh}^{n*}\right)/\left(1 - S_{wrh}^{n*}\right)\right] \ldots\ldots\ldots (27)$

with $S_{wrh}^{n*} = \left[\dfrac{k_{rw}^{PD}}{1 + \left(1 - k_{rw}^{PD}\right)c_{wh5}}\right]^{1/c_{wh4}}, \quad \ldots\ldots\ldots (28)$

where the primary-drainage curve (Eq. 9) is the same for both systems and the water/hydrocarbon parameters are interpolated as

$$c_{wh4} = c_{wg4} + f_h\left(c_{wo4} - c_{wg4}\right) \ldots\ldots\ldots (29)$$

and $c_{wh5} = c_{wg5} + f_h\left(c_{wo5} - c_{wg5}\right). \quad \ldots\ldots\ldots (30)$

Because there is no hysteresis of the water relative permeability in the water/gas system, $c_{wg4} = c_{w1}$ and $c_{wg5} = 0$. When water/gas data are not available oil/gas data treated as a function of liquid saturation can be used as an approximation because they are usually strongly wetting and approximately the same as the water/gas data.

Three-Phase Relative Permeability

Virtually no true three-phase data are available for Prudhoe Bay. There are, however, a number of two-phase experiments with residual third phase present.

Effect of Trapped Gas on Residual Oil. For water-wet rock, literature data[12] show that ROS's decrease in the presence of trapped gas by approximately half the trapped-gas saturation for gas saturations less than 20%. Prudhoe Bay shows a much weaker dependence, largely because of the mixed-wet nature of the reservoir. For example, the waterflood ROS measured on a composite was 25%; after resaturation and subsequent gasflood waterflood the trapped-gas saturation was 23% and the ROS was 22%. Thus, the reduction in ROS is approximately 13% of the trapped-gas level.

Fig. 7 shows oil relative permeability for three composites. For a water-wet rock, one would expect oil relative permeability to be a function of gas and oil saturation [because gas and oil would compete for the same (large) pores] and water relative permeability to be a function of only water saturation. As a result, in strongly water-wet rock, ROS is decreased by trapped gas. Prudhoe data show that oil relative permeability is nearly a function of oil saturation (over the range of saturations investigated, Fig. 7), while the water relative permeability is diminished by the presence of gas (**Fig. 8**). (Data from Fig. 8 are erratic at low water saturations because water relative permeability in displacement tests is sensitive to core-scale heterogeneities; data at higher water saturations are more reliable.) This behavior can be understood in terms of the weakly mixed-wet nature of Prudhoe rock. Normally, in a strongly water-wet rock, water enters the smaller pores first owing to capillarity. However, in a mixed-wet rock, most of the water will invade the larger pores first and then the smaller pores. In addition, water flows into the pores that provide the least resistance to flow, the larger pores. Thus, gas and water compete for the larger pores, leaving the oil less affected in the intermediate-sized pores. By extrapolating the oil relative permeability curves in Fig. 7 to low oil saturations, we infer that the ultimate residual oil is weakly affected by trapped-gas saturation. The net impact of addition of trapped gas is to decrease the water/oil

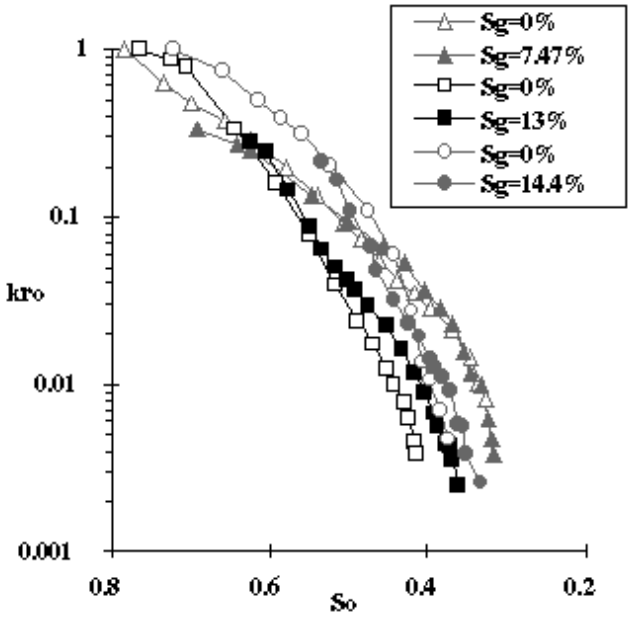

Fig. 7—Effect of trapped gas on oil relative permeability.

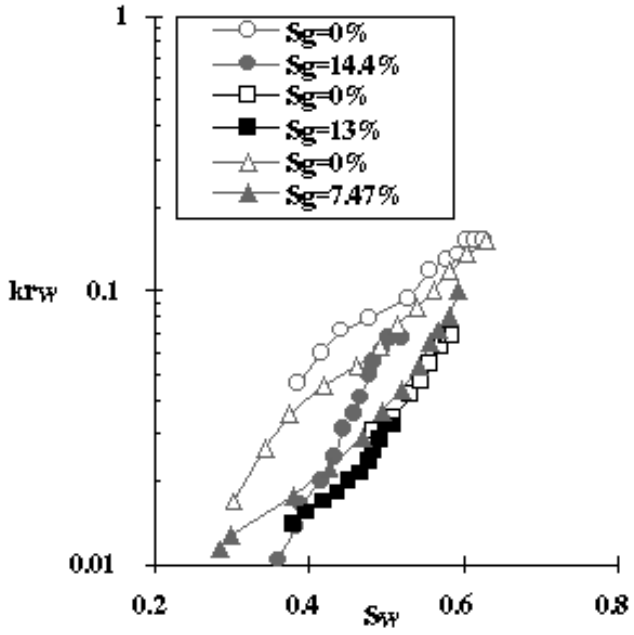

Fig. 8—Effect of trapped gas on water relative permeability.

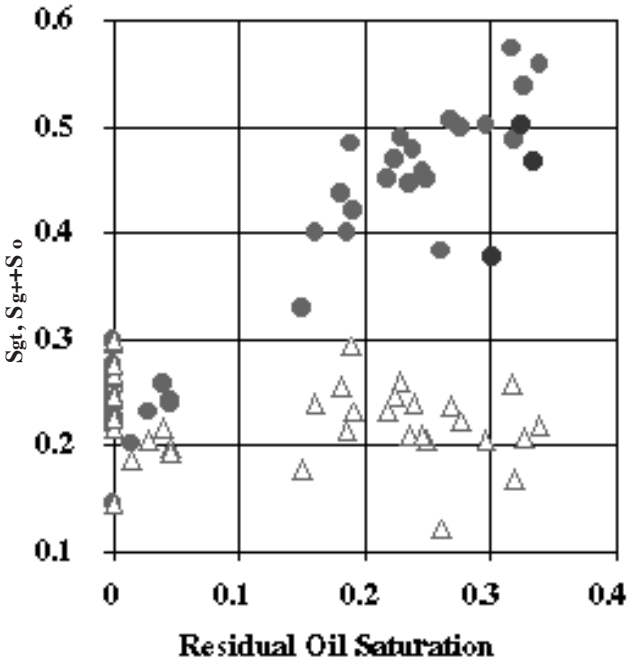

Fig. 9—Prudhoe Bay laboratory data demonstrating that the sum of the trapped-gas saturation and ROS (closed symbols) can be greater than trapped-gas saturation (open symbols).

relative permeability ratio and thus improve oil recovery after a few pore volumes (PV's) of throughput.

The effective residual oil after a few PV's of throughput is reduced primarily because of the reduction of water saturation and water mobility created by the presence of gas (Fig. 8). The lower water mobility drives the oil saturation to lower values than would otherwise be the case for waterflooding with no gas present. Because oil relative permeability is nearly a function of oil saturation and water relative permeability decreases in the presence of trapped gas, the net effect is to provide a lower total mobility than would be predicted if water relative permeability were taken to be just a function of water saturation. Therefore, oil relative permeability increases in the presence of trapped gas, as is often assumed in conventional three-phase relative permeability models.

Effect of Residual Oil on Trapped Gas. The data in **Fig. 9** (open triangles) show that the trapped-gas saturation is essentially independent of ROS. The experiments were waterfloods with varying amounts of oil and mobile gas initially present, including many waterfloods with water displacing gas with residual oil present. For a strongly water-wet system, both oil and gas compete for the larger pores. One would, therefore, expect some tradeoff between trapped gas and oil. For a weakly mixed-wet rock, such as the Sadlerochit, the oil is trapped mainly in kaolinite clay booklets or as thin films. Thus, the trapped gas and residual oil should be approximately independent because they are not competing for the same pores. The data largely confirm this, with only a small interaction noticeable.

Sum of ROS and Trapped-Gas Saturation. Simultaneous trapping of oil and gas by water happens at the tail end of the multicontact miscible gas process because of the crossflow of oil and in other high IFT circumstances. Fig. 9 shows Prudhoe laboratory data that indicate that the trapped-gas saturation is essentially independent of ROS; as a result, the sum of the two saturations can exceed 50%. Similar experiments run on restored core to understand the impact of trapped gas on waterflood ROS showed little dependence of residual oil on trapped gas and therefore a similar value for the sum of the trapped-gas and ROS's. The data do not support correlations that predict that the sum of the oil and gas residuals is a constant. **Fig. 10** shows that this observation is true for a wide range of reservoirs and that the sum of the trapped-gas and ROS's tends to increase with two-phase ROS to waterflood.

Fig. 11 shows log-calculated hydrocarbon saturations from a cored well near a WAG injector.[19] Data (abscissa) are for plug samples and for two different levels of inferred trapped-gas saturation, greater than 20% and between 15 and 20%. Gas saturation is inferred by subtracting the oil saturation, calculated from stock-tank-oil saturation measured on cores and corrected for bleeding and shrinkage, from the total hydrocarbon saturation calculated from logs. Only higher gas saturations were used to focus on well-swept layers rather than averaging partially and well-swept layers. The data were also high-graded to eliminate conglomeratic samples and samples with less than 10-md

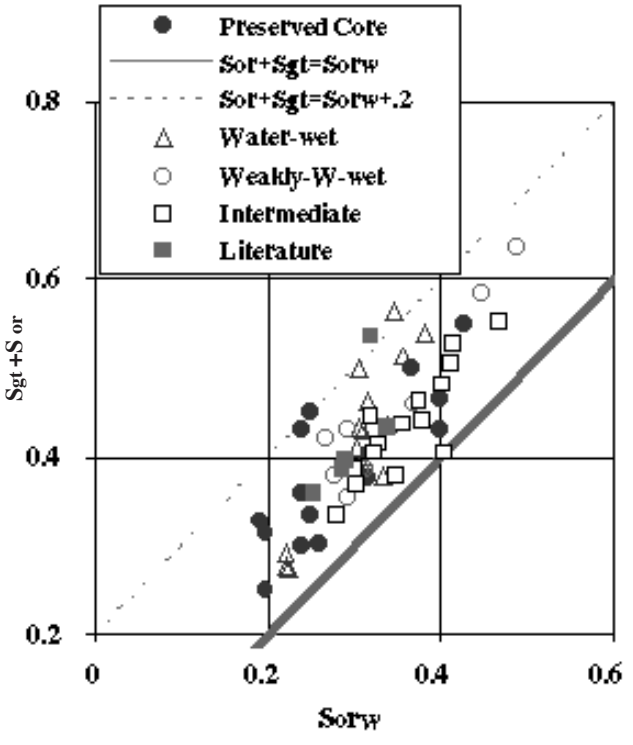

Fig. 10—Data showing how the sum of trapped-gas saturation and ROS depends on (waterflood) residual-oil level. Data are from a wide variety of fields, including Prudhoe Bay.

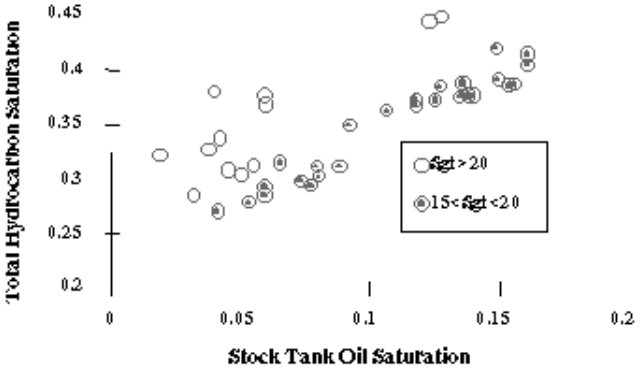

Fig. 11—Log-calculated hydrocarbon saturations from DS 3-18i vs. stock-tank-oil saturation from core. The sum of trapped-gas saturation and ROS is frequently greater than 25% and increases nearly linearly with oil saturation, indicating that they are largely independent.

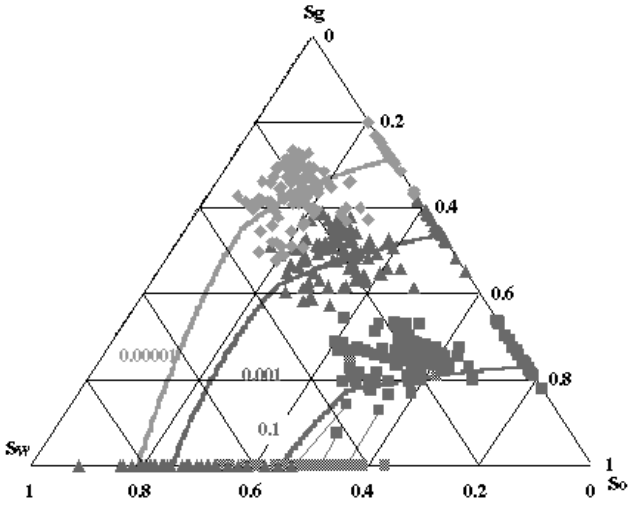

Fig. 12—Three-phase oil relative permeability isoperms predicted with new correlation. Data are centrifuge oil relative permeability displaced by gas or water and waterflood experiments in the presence of trapped gas.

permeability and 15% porosity because these samples are likely not to be well-swept and are more likely to be subject to artifacts in log or core analysis. The sum of the hydrocarbon phases extends into the low forties and is approximately linear in stock-tank-oil saturation, indicating that the trapping of oil is basically independent of the trapping of gas. This implies that it is possible to have 20% trapped oil along with trapped gas.

Effect of Initial Water on k_{rog}. Review of the literature indicates that the presence of initial water is generally thought to increase oil recovery from gravity drainage up to the point where water becomes mobile, when oil recovery begins to decrease. Many authors[8,22] have found that oil relative permeability is essentially a function of gas or total liquid saturation, independent of initial water saturation. These results imply that the sum of ROS and initial water saturation should be a constant. Consequently, ROS is strongly dependent on initial water saturation and recovery efficiency should increase with increasing initial water saturation. This picture characterizes Prudhoe Bay oil relative permeability at moderate and high, but not low, liquid saturations.

Fig. 12 shows oil relative permeability isoperms derived from centrifuge measurements on plugs. The isoperms show that oil relative permeability is approximately a function of liquid saturation alone at higher oil saturations or high oil relative permeability as long as water is not mobile ($S_w < 0.3, S_l > 0.6$). A constant liquid saturation approximation is nearly adequate even at relative permeability levels as low as $k_{rog} = 0.004$. At low oil saturations and at sufficiently high water saturations, oil relative permeability depends only on oil saturation. This is consistent with the idea that oil flow is dominated by the thickness of the oil film between water and gas at low oil saturations, but when oil films are thick, oil relative permeability is unaffected by the presence of water. Additionally, the larger pores contribute more to hydraulic conductance, according to a relationship of pore size to a power of at least two but probably three or more. At large oil saturations, the contribution of small pores (i.e., those that may be occupied by oil or water depending on the initial water saturation level) is insignificant and the presence or absence of oil in those pores has negligible impact on oil relative permeability. In the limit of low water saturations, water is in the microporosity and does not impact the relative permeability of oil; however, because oil is also in the microporosity, it does impact oil saturation. As a result, oil relative permeability depends mainly on total liquid saturation in the limit of low water and high oil saturations. When the oil saturation is very low, oil relative permeability becomes nearly independent of water saturation because oil spreads on the gas/water interface and in the limit of no oil saturation the flow must be zero. Residual oil to gas found from capillary pressure data at very high levels of capillary pressure also shows that residual oil to gas is nearly independent of initial water saturation.

Three-Phase Compositional Functions. The three-phase oil relative permeability equation is similar to Stone I but slightly more general.

$$k_{ro} = k_{roo}(S_o)\frac{k_{rog}(1 - S_g)k_{rhw}(1 - S_w)}{k_{roo}(1 - S_g)k_{roo}(1 - S_w)}. \quad \ldots\ldots\ldots\ldots (31)$$

This slightly more general form allows the three-phase oil relative permeability to be independent of the other two phase saturations if the dependence of oil relative permeability on oil saturation in the gas/oil system is identical to the dependence of oil relative permeability in the water/oil system and the three-phase k_{roo} function also has the same dependence on oil saturation. Oil isoperms have also been reported as straight lines to within the accuracy of the data for water-wet systems. The oil phase equation reduces to Stone I if $k_{roo} = S_o$. A slightly simpler function is used for gas.

$$k_{rg} = k_{rgg}(S_g)\frac{k_{rhw}(1 - S_w)}{k_{rgg}(1 - S_w)}. \quad \ldots\ldots\ldots\ldots\ldots\ldots (32)$$

The three-phase "*oo*" functions have the same general form as the two-phase oil relative permeability functions.

$$k_{roo}(S) = \left(\frac{S - \theta S_{ot}}{1 - \theta S_{ot}}\right)^{\theta c_{01} + (1-\theta)}, \quad \ldots\ldots\ldots\ldots\ldots (33)$$

$$\text{where } S_{ot} = S_{otw} + \frac{(S_{oot} - S_{otw})S_g}{\left[1 - \max(S_{org}, S_{wi} + S_{oot})\right]} \quad \ldots\ldots\ldots (34)$$

$$\text{and } S_{oot} = \frac{(1 - S_w^{\min})}{1 + (1/S_{or} - 1)(1 - S_w^{\min})^{1/(1-S_{or})}}. \quad \ldots\ldots\ldots (35)$$

Two-phase oil relative permeability in the gas/oil system has a similar form.

$$k_{rog}(1 - S_g) = \left(\frac{1 - S_g - \theta S_{org}}{1 - \theta S_{org}}\right)^{\theta c_{og1} + (1-\theta)}. \quad \ldots\ldots\ldots (36)$$

The three-phase "*gg*" have the same form as two-phase gas relative permeability function,

$$k_{rgg}(S_g) = \frac{\left(1 + \theta c_{g2}\right)S_{gg}^{\theta c_{g1} + (1-\theta)}}{\left(1 + \theta c_{g2} S_{gg}^{\theta c_{g3}}\right)}, \quad \ldots\ldots\ldots\ldots\ldots (37)$$

$$\text{with } S_{gg}(S_g) = \left[(S_g - \theta S_{gt})/(1 - \theta S_{gr})\right]. \quad \ldots\ldots\ldots\ldots (38)$$

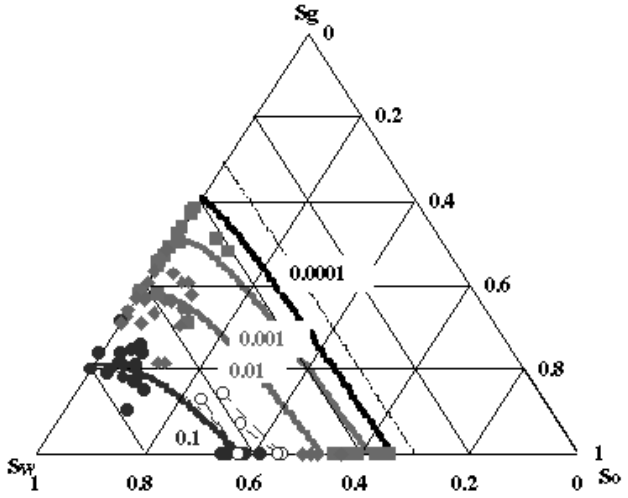

Fig. 13—Water relative permeability isoperms $S_{wc} = 0.3$, predicted by correlation, compared with data. Data with connecting dotted lines show the same sample with and without trapped gas.

The Corey exponents and parameters are scaled with capillary number from immiscible values so that the proper miscible limit is approached. Trapping of gas by oil occurs as a result of capillary phenomena and disappears as miscibility is approached. As a result, oil and gas phase relative permeability increase as miscibility is approached. Oil and gas relative permeability isoperms become symmetrical about the line $S_g = S_o$ as miscibility is approached.

A simple saturation-weighted average of the water relative permeabilities from the water/oil and water/gas systems; i.e.,

$$k_{rw} = \left[S_o k_{rwh}(S_w, f_o) + S_g k_{rwh}(S_w, f_g)\right]/(S_o + S_g) \quad \ldots\ldots\ldots (39)$$

was found to capture the basic feature that water relative permeability depends on gas saturation in a mixed-wet rock and agrees with available data (**Fig. 13**). Water/gas data in the presence of S_{orm} and a limited amount of water/oil data in the presence of trapped gas were used for validation.

Measurements of water relative permeability during waterfloods and miscible WAG floods performed on the same composites show systematic differences. In one waterflood, $k_{rwo}(S_w = 0.792) = 0.311$, whereas in the subsequent WAG $k_{rw}(S_w = 0.819, S_{orm} = 0.026) = 0.071$. In a second test, $k_{rwo}(S_w = 0.75) = 0.27$, whereas $k_{rw}(S_w = 0.779, S_{orm} = 0.054) = 0.077$. Another three samples had average values of $k_{rw}(S_{or} = 0.277) = 0.32$ and $k_{rw}(S_{gt} = 0.277, S_{orm} = 0.043) = 0.07$.

This simple three-phase model reduces to the proper limiting cases as expected. If either hydrocarbon saturation is zero, the water relative permeability of the other phase is recovered. As miscibility is approached, both water/hydrocarbon relative permeability two-phase limits approach each other and the resulting relative permeability is a function of only water saturation. In addition, if the two sets of two-phase curves are the same, the water relative permeability depends only on water-saturation as it does in strongly wetting systems. Most importantly, it predicts that trapped gas will lead to lower water mobility and higher oil recovery efficiency.

Discussion

The correlation presented is designed to be a general-purpose model to incorporate the range of recovery mechanisms seen at Prudhoe Bay. However, the most interesting applications have been to the multicontact miscible gas process where the full range of features are used. It and similar schemes have been used extensively in compositional simulation of the miscible gasflooding.[19,20,25] When used with fine-scale reservoir descriptions, it has produced a suitable match to the available field data that from a fiberglass encased observation well[25] and an infill well with compositional analysis[19] as well as produced-oil and gas/oil ratio. It is difficult to generalize about the magnitude of the impact of the compositional dependence because results depend on the reservoir description, slug size, WAG ratio, and other process parameters. Realistic simulations at Prudhoe Bay conditions indicate that including IFT or capillary number dependence changes the incremental EOR recovery by less than 2% of the incremental recovery. Including the dependence of water relative permeability on gas saturation can increase the projected incremental by 8 to 15% of the incremental and is largest in oil-wet situations. The choice of parameters used in interpolating between oil/water and gas/water relative permeability can also impact recovery with a 15% variation in predicted recovery for realistic choices of parameters. For a given description, the incremental recovery can vary by $\pm 20\%$ of the average incremental, depending on the initial water saturation level and implied wettability.

Conclusions

1. The correlation presented demonstrates a practical way of including the important relative permeability mechanisms in a compositional simulation, which consistently treats compositional variation, hysteresis, and trapping.

2. The relative permeability mechanisms that are important to predicting EOR performance at Prudhoe Bay are largely immiscible and included (3) dependence of water/oil relative permeability on minimum water saturation, both because in any mixed-wet rock water/oil relative permeability depends on minimum water saturation and because the wettability depends on initial water saturation at Prudhoe; (2) three-phase relative permeability, which includes water relative permeability that depends on gas as well as water saturation, while oil relative permeability is nearly independent of gas saturation; and (3) the trapping of gas by water and/or oil.

3. For the immiscible conditions typically encountered during cross-flow in the miscible process the sum of trapped gas and ROS can be greater than either ROS or trapped-gas saturation.

Nomenclature

c_{ijk} = kth parameter in i-phase/j-phase relative permeability equation
f = function representing the composition dependence
k = absolute permeability, L^2, md
k_{rocw} = relative permeability to oil at initial water
k_{ri} = relative permeability for i phase
k_{rij} = relative permeability of i phase with relation to j phase
N_c = capillary number
S_i = saturation of Phase i
S_{gc} = critical gas saturation
$S_g^{\max}$ = maximum gas saturation
S_{ir} = maximum trapped i-phase saturation
S_{irj} = maximum residual of Phase i with relation to Phase j
S_{itk} = residual of Phase i with relation to Phase j
S_{nr}^0 = low N_c limit of nonwetting-phase residual
S_{orm} = residual-oil miscible flood
S = initial water saturation
$S_w^{\min}$ = minimum water saturation
∇p = pressure gradient
θ = function describing N_c dependence, Eq. 11.
σ = IFT
ξ_h = parachor-weighted molar density for Phase h

Acknowledgments

I thank Arco Alaska Inc. and the working-interest owners of Prudhoe Bay for permission to publish this paper. A wide variety of data discussed in this paper was measured by the various companies participating in the Prudhoe Bay Unit. The results of this work would not be possible without the work of numerous people in these companies. I thank Jake Rathmell, Fred Stalkup, Andy Spence, Richard Treinen, and Jim Kralik for their support and many helpful suggestions in data interpretation. The interpretations and conclusions presented in this paper are those of the author and do not necessarily reflect the opinions of all the Prudhoe Bay working-interest owners.

References

1. Abrams, A.: "The Influence of Fluid Viscosity, Interfacial Tension, and Flow Velocity on Residual Oil Saturation Left by Waterflood," *SPEJ* (October 1975) 437.
2. Asar, H. and Handy, L.L.: 1988 "Influence of Interfacial Tensions on Gas/Oil Relative Permeabilities in a Gas-Condensate System," *SPERE* (February 1988) 257.
3. Baker, L.E.: "Three-Phase Relative Permeability Correlations," paper SPE 17369 paper presented at the 1988 SPE/DOE EOR Symposium, Tulsa, Oklahoma, 17–20 April.
4. Bardon, C. and Longeron, D.: "Influence of Very Low Interfacial Tensions on Relative Permeability," *SPEJ* (October 1978) 391.
5. Carlson, F.M.: "Simulation of Relative Permeability Hysteresis to the Nonwetting Phase," paper SPE 10157 presented at the 1981 SPE Annual Technical Conference and Exhibition, San Antonio, Texas.
6. Chierici, G.L., Ciucci, G.M., and Long, G.: "Experimental Research on Gas Saturation Behind the Water Front in Gas Reservoirs Subjected to Water Drive," *Proc*., Sixth World Petroleum Congress (1963) 483.
7. Corey, A.T.: "The Interrelation Between Gas and Oil Relative Permeabilities," *Producers Monthly* (November 1954) 38.
8. Delclaud, J., Rochon, J., and Nectoux, A.: "Investigation of Gas/Oil Relative Permeabilities: High-Permeability Oil Reservoir Application," paper SPE 16966 presented at the 1987 SPE Annual Technical Conference and Exhibition, Dallas, 27–30 September.
9. Dria, D.E., Pope, G.A., and Sepehrnoori: "Three-Phase Gas/Oil Relative Permeabilities Measured Under CO_2 Flooding Conditions," *SPERE* (May 1993)143.
10. Fayers, F.J. and Matthews, J.D.: "Evaluation of Normalized Stones' Methods for Estimating Three-Phase Relative Permeabilities," *SPEJ* (April 1984) 224.
11. Geffen, T.M. *et al*.: "Efficiency of Gas Displacement from Porous Media by Liquid Flooding," *Trans*., AIME (1952) **195,** 29.
12. Holmgren, C.R. and Morse, R.A.: "Effect of Free Gas Saturation on Oil Recovery by Water Flooding," *Trans*., AIME (1951) **192,** 135.
13. Jerauld, G.R.: "Gas/Oil Relative Permeability of Prudhoe Bay," *SPERE* (February 1996) 66.
14. Jerauld, G.R. and Rathmell, J.J.: "Wettability and Relative Permeability of Prudhoe Bay: A Case Study In Mixed-Wet Reservoirs," *SPERE* (February 1994) 58.
15. Jerauld, G.R. and Salter, S.J.: "The Effect of Pore-Structure on Hysteresis in Relative Permeability and Capillary Pressure: Pore-Level Modeling," *Transport in Porous Media* (1990) 103.
16. King, M.J.: "Simultaneous Determination of Residual Saturation and Capillary Pressure Curves Utilizing the Ultracentrifuge," paper SPE 15595 presented at the 1986 SPE Annual Technical Conference and Exhibition, New Orleans, 5–6 October.
17. Lake, L.W.: *Enhanced Oil Recovery*, Prentice Hall Inc., Englewood Cliffs, New Jersey (1989).
18. Land, C.S.: "Comparison of Calculated With Experimental Imbibition Relative Permeability," paper SPE 3360 presented at the 1971 SPE Rocky Mountain Regional Meeting, Billings, Montana, 2–4 June.
19. McGuire, P.L. *et al*.: "Core Acquisition and Analysis for Optimization of the Prudhoe Bay Miscible Gas Project," *SPERE* (May) 94–99.
20. McGuire, P.L. and Stalkup, F.I.: "Performance Analysis and Optimization of the Prudhoe Bay Miscible Gas Project," *SPERE* (May 1995) 88.
21. McKay, B.A.: "Laboratory Studies of Gas Displacement from Sandstone Reservoirs having Strong Water Drive," *APEA J*. (1974) 189.
22. Owens, W.W., Parrish, R., and Lamoreaux, W.E.: "An Evaluation of a Gas Drive Method for Determining Relative Permeability Relationships," *Trans*., AIME (1956) **207,** 275.
23. Reid, R.C., Prausnitz, J.M., and Poling, B.E.: *The Properties of Gases and Liquids,* McGraw-Hill, New York City (1986).
24. Salathiel, R.A.: "Oil Recovery by Surface Film Drainage in Mixed-Wettability Rocks," *JPT* (October 1973) 1216.
25. Stalkup, F.I. and Crane, S.D.: "Reservoir Description Detail Required to Predict Solvent and Water Saturations at an Observation Well," *SPERE* (February 1994) 35; *Trans*., AIME, **297.**
26. Stern, D.: "Mechanisms of Miscible Oil Recovery: Effects of Pore-Level Fluid Distribution," paper SPE 22652 presented at the 1991 SPE Annual Technical Conference and Exhibition, Dallas.
27. Stone, H.L.: "Probability Model for Estimating Three-Phase Relative Permeability," *JPT* (February 1970) 214.

SI Metric Conversion Factors

cp	$\times 1.0^*$	$E-03 = Pa \cdot s$
dyne/cm	$\times 1.0^*$	$E+00 = mN/m$
ft	$\times 3.048^*$	$E-01 = m$
°F	$(°F-32)/1.8$	$= °C$
md	$\times 9.869\ 233$	$E-04 = \mu m^2$
psi	$\times 6.894\ 757$	$E+00 = kPa$

*Conversion factor is exact.

SPERE

Gary Jerauld is a senior principal research engineer in the Gas EOR Processes Group of Arco E&P Technology. His research interests are in multiphase flow in porous media including wettability, relative permeability, pore-level modeling, near-miscible gas injection processes, and scale-up. Jerauld holds a BS degree from Rensselaer Polytechnical Inst. and a PhD degree from the U. of Minnesota, both in chemical engineering.